Long-lived circularly-polarized phosphorescence in helicene-NHC-rhenium(I) complexes: The influence of helicene, halogen and stereochemistry on emission properties

Etienne S Gauthier, Laura Abella, Nora Hellou, Benoît Darquié, Elsa Caytan, Thierry Roisnel, Nicolas Vanthuyne, Ludovic Favereau, Monika Srebro-Hooper, J a Gareth Williams, et al.

Long-lived circularly-polarized phosphorescence in helicene-NHC -rhenium(I) complexes: the influence of helicene, halogen and stereochemistry on emission properties

Etienne S. Gauthier,[a] Laura Abella,[b] Nora Hellou,[a] Benoît Darquié,[c] Elsa Caytan,[a] Thierry Roisnel,[a] Nicolas Vanthuyne,[d] Ludovic Favereau,[a] Monika Srebro-Hooper,[e] J. A. Gareth Williams,*[f] Jochen Autschbach*[b] and Jeanne Crassous*[a]

[a] Etienne S. Gauthier, Dr. Nora Hellou, Dr. Elsa Caytan, Dr. Thierry Roisnel, Dr. Ludovic Favereau, Dr. Jeanne Crassous
Univ Rennes, CNRS, ISCR - UMR 6226,
F-35000 Rennes, France.
E-mail: jeanne.crassous@univ-rennes1.fr
[b] Dr. Laura Abella, Prof. Jochen Autschbach
Department of Chemistry, University at Buffalo,
State University of New York, Buffalo, New York 14260, USA.
E-mail: jochena@buffalo.edu
[c] Dr. Benoît Darquié
Laboratoire de Physique des Lasers, Université Paris 13, Sorbonne Paris Cité, CNRS, Villetaneuse, France.
[d] Dr. Nicolas Vanthuyne
Aix Marseille University, CNRS Centrale Marseille, iSm2, 13284 Marseille, France.
[e] Dr. Monika Srebro-Hooper
Faculty of Chemistry, Jagiellonian University, Gronostajowa 2, 30-387 Krakow, Poland.
[f] Prof. J. A. Gareth Williams
Department of Chemistry, Durham University, Durham, DH1 3LE, U.K.
E-mail: j.a.g.williams@durham.ac.uk

Abstract: First enantiopure, chiral-at-rhenium complexes of the form *fac*-ReX(CO)$_3$(:C^N) have been prepared, where :C^N is a helicene N-heterocyclic carbene ligand and X = Cl or I. They have shown strong changes in the emission characteristics, notably strongly enhanced phosphorescence lifetimes (reaching 0.7 ms) and increased CPL activity, as compared to their parent chiral models lacking the helicene unit. Identity of the halogen along with its position within the dissymmetric stereochemical environment strongly affect the photophysics of the proposed complexes, particularly the phosphorescence quantum yield and lifetime. All these results give fresh insight into fine tuning of photophysical and chiroptical properties of Re-NHC systems.

N-Heterocyclic carbenes (NHCs) are important ligands for organometallic and coordination chemistry[1] due to their strong σ-donor abilities that result in the formation of stable metal−carbon bonds. NHC ligands have been applied widely in homogeneous catalysis,[2] and more recently in materials science.[3] Many classes of luminescent M-NHC complexes have been developed, with M = Pt,[4a] Ir,[4b] Ru[4c], Au,[4d] Ag,[4d,e] Cu,[4d,f,g] or Fe,[4h] that display potential applications in photonic and optoelectronic devices, in bioimaging and cancer therapy, or as photosensitizers in photoredox catalysis. Recently,[5] neutral d^6-rhenium(I) complexes of the form *fac*-ReX(CO)$_3$(:C^N) have been prepared. Here, X is a halogen and :C^N is a bidentate ligand related to bipyridine but incorporating an imidazolylidene NHC fragment substituted with an N-coordinating unit. Related photophysical studies highlight an undesirable influence of the NHC ligand in such Re(I) complexes, with a dramatic decrease of both the excited-state lifetime and the luminescence quantum yield, hampering the potential of such compounds in the context of the aforementioned applications.[6]

Our group has recently developed chiral versions of several different classes of organometallic compounds[7] by incorporating helicenes[8] as ancillary ligands and NHC-based complexes with intriguing emission properties have been addressed.[9] Here, we describe the first chiral NHC-Re(I) complexes bearing both helical and metal-centered stereogenic elements. Enantiopure complexes of the form *fac*-ReX(CO)$_3$(:C^N) have been prepared, where the NHC ligand incorporates a [5]helicene unit, and X is either iodine (**A**^{1,2}) or chlorine (**B**^{1,2}) (Figure 1). Their photophysical (absorption and emission) and chiroptical properties (optical rotation - OR, electronic circular dichroism - ECD, and circularly polarized emission - CPL) have been studied both experimentally and theoretically. Model complexes **C**-**E**, featuring achiral benzimidazole and imidazole-based NHC ligands and chirality only limited to the rhenium center, have been studied for comparison (Figure 1). To our knowledge, no enantiopure rhenium complex based on an NHC ligand has been reported up to now. It was therefore of great interest to: *i*) prepare enantiopure, 'chiral-at-metal' Re(I) complexes bearing a helicene-NHC-pyridyl ligand; *ii*) study the influence of helical NHC ligands on the photophysics of the complexes, especially their emission properties; and *iii*) examine the resulting CPL activity. Very surprisingly, we observed that the helical π-conjugated nature of the NHC ligand, and the identity of the halogen, along with its position within the dissymmetric helical environment, all have a profound influence on the photophysics of the proposed complexes. The influence on the phosphorescence quantum yield and lifetime is particularly strong, affording new insights into the photophysical properties of Re-NHC complexes. Subtle chemical and stereochemical changes may thus lead to profound effects on the photophysics. In particular, efficient long-lived CPL activity can be obtained by controlling all of these parameters.

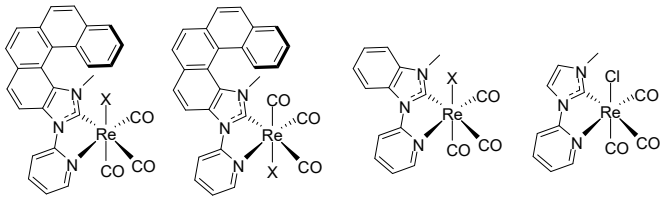

(*M*,*A*$_{Re}$) [and (*P*,*C*$_{Re}$)] **A**^{1} (X = I), **B**^{1} (X = Cl) | (*M*,*C*$_{Re}$) [and (*P*,*A*$_{Re}$)] **A**^{2} (X = I), **B**^{2} (X = Cl) | *A*$_{Re}$ [and *C*$_{Re}$] **C** (X = I), **D** (X = Cl) | *A*$_{Re}$ [and *C*$_{Re}$] **E**

Figure 1. Chiral helicene-NHC Re complexes and models studied in this work.

As depicted in Scheme 1, the synthesis started from [5]helicene-imidazole **1**, whose preparation we have reported previously.[9] This compound was subjected to Ullmann-type coupling with 2-bromopyridine, using CuI/L-proline as the catalytic system,[10] to yield 3*N*-(2-pyridyl)-[5]helicene-imidazole **2**. Methylation with MeI in acetonitrile gave imidazolium iodide salt **3**, from which the corresponding chloride salt **4** was obtained by anion metathesis on a Dowex resin. Compounds **1**-**4** and the final products were fully characterized by ^{1}H and ^{13}C NMR spectroscopy and mass spectrometry (all details are provided in the Supporting Information, SI). Following literature procedures,[5] salts **3** and **4** were then used to obtain the iodo and chloro rhenium complexes **A** and **B**, respectively. The iodo derivatives **A**^{1,2} were prepared directly from the iodide salt **3** employing $ReCl(CO)_5$ as the Re source and K_2CO_3 as the base for the *in situ* generation of the carbene, in refluxing toluene, with 65% yield. The chloro analogues **B**^{1,2} were obtained in a similar way from chloride salt **4** in 54% yield. Notably, the ^{1}H NMR spectra of the d^6-Re(I) compounds revealed the loss of the precarbenic proton and the appearance of two sets of signals corresponding to two diastereoisomers (in ratios of 83:17 for **A**^{1,2} and 67:33 for **B**^{1,2}, as further confirmed by HPLC), thus suggesting

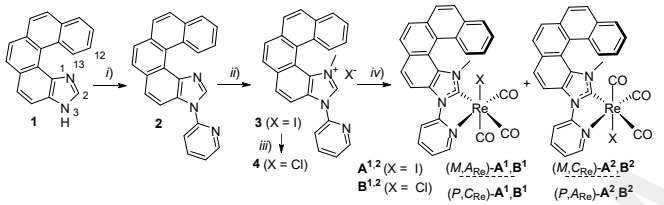

Scheme 1. Synthetic access to helicene-NHC-Re complexes **A** and **B**. *i*) 2-Br-pyridine, K_2CO_3, CuI (cat.), L-Pro (cat.), DMSO, 110°C, 63 h; 69%; *ii*) MeI, MeCN, reflux, overnight; 83% (2 steps); *iii*) Dowex resin, acetone; 88%; *iv*) $ReCl(CO)_5$, K_2CO_3, toluene, reflux, 22 h; 65% (**A**^{1,2}), 54% (**B**^{1,2}).

substantial diastereoselectivity upon coordination of the helicene ligand to the metal. Indeed, both **A** and **B** contain two stereogenic elements: the [5]helicene – which is configurationally stable thanks to the methyl group at the N^1 atom – and the Re(I) center, which can adopt *A*/*C* stereochemistry[11] (see Scheme 1 and SI). Consequently, mixtures of diastereomeric complexes (*M*,*A*$_{Re}$)-**A**^{1}/**B**^{1} and (*M*,*C*$_{Re}$)-**A**^{2}/**B**^{2} are formed {together with their mirror images (*P*,*C*$_{Re}$)-**A**^{1}/**B**^{1} and (*P*,*A*$_{Re}$)-**A**^{2}/**B**^{2}, respectively}.

The structure of the complexes was further evidenced by X-ray crystallography of single crystals of the minor diastereoisomer **A**^{2}. It crystallized in the *P*2$_1$/n centrosymmetric space group and corresponded to the (*M*,*C*$_{Re}$)/(*P*,*A*$_{Re}$)-**A**^{2} enantiomeric pair, as depicted in the heterochiral assembly in Figure 2. In **A**^{2}, the Re(I) ion adopts a slightly distorted pseudo-octahedral geometry, with the three carbonyl groups being *fac*-oriented around the metal.[5] The equatorial planes are defined by the chelating pyridine-NHC ligand and two carbonyls, with the third carbonyl and the iodine atom occupying the axial positions. The iodine points in the opposite direction to the helicene moiety in **A**^{2}, while in the major diastereomer (*M*,*A*$_{Re}$)/(*P*,*C*$_{Re}$)-**A**^{1}, it is directed towards the helicene core. The helicenic moiety displays a helicity angle of 51.23°, typical for [5]helicenes and consistent with that measured for a cycloiridiated complex bearing a similar [5]helicene-NHC ligand.[9] The chelating pyridine and NHC rings are almost coplanar (NCNC dihedral angle of 3.54°), and the Re-N$_{pyridine}$, Re-C$_{carbene}$, and Re-I bond lengths are respectively 2.206, 2.124, and 2.789 Å.[5] All these observations indicate extended π-conjugation over the whole molecule and efficient electronic interaction between the bidentate [5]helicene-NHC-pyridyl ligand and the metal, as corroborated by isosurfaces of frontier molecular orbitals (MOs, *vide infra*) and results of charge and bonding-energy decomposition analysis[12] of the compounds (see SI). Single crystals of (*P*,*A*$_{Re}$)-**B**^{2}, **C**, (+)-**D** and (-)-**E** were also grown using the same technique as for **A**^{2}, and analyzed by X-ray crystallography (see SI).

As neutral, stable species, complexes **A**^{1,2} and **B**^{1,2} were readily obtained in diastereomerically and enantiomerically pure forms. Indeed, enantiopure samples (with *ee* 97–99.5%) of (*M*,*A*$_{Re}$)/(*P*,*C*$_{Re}$)-**A**^{1} and (*M*,*C*$_{Re}$)/(*P*,*A*$_{Re}$)-**A**^{2}, and of (*M*,*A*$_{Re}$)/(*P*,*C*$_{Re}$)-**B**^{1} and (*M*,*C*$_{Re}$)/(*P*,*A*$_{Re}$)-**B**^{2}, were obtained *via* HPLC over a chiral stationary phase (see SI). For comparison, three model systems were also examined: the iodo Re-NHC complex **C**, its chloro analogue **D**, and chloro Re-NHC compound **E** lacking the phenyl ring in the NHC unit (Figure 1). Although the synthesis and photophysics of **D** and **E** have been described, there is no precedent with regard to their chiroptical properties. Complex **C** has not been reported previously. Compounds **C**, **D** and **E**, prepared by adapted literature procedures,[5] have therefore been resolved into pure *A*$_{Re}$/*C*$_{Re}$ enantiomers by chiral HPLC separations (*ee* > 98%, see SI). X-ray crystallography analysis of (-)-**E** (*P*21 space group) enabled its assignment as the (*A*$_{Re}$)-(-)- and (*C*$_{Re}$)-(+)-**E** stereochemistries (Figure 2).

The UV-vis absorption spectra of the Re-NHC complexes **A**-**E** were studied experimentally (in CH_2Cl_2 at around 10^{-4} M) and theoretically, *via* (TD-)DFT calculations, using Gaussian 16,[13] the PBE0 functional,[14] the def2-SV(P) basis for lighter atoms and the SDD basis with matching relativistic core potentials for Re and I,[15] and with the polarizable continuum model[16] (PCM) for the solvent CH_2Cl_2 (see SI). As previously reported,[5b] Re-NHC-Cl **D** and **E** compounds display two dominant bands that are attributable to $\pi \rightarrow \pi^*$ transitions below 300 nm, and a mixture of metal-to-ligand (ML) and intraligand (IL) charge-transfer (CT) excitations between 330 and 440 nm (here and in the following text, L corresponds to the :C^N ligand; see also Table S2.1, Figure S2.4). Similar features are found for the new Re-I complex **C** (see SI and Table 1). [5]Helicene-NHC-based complexes **A** and **B** display overall more intense and more structured bands. Re-I systems **A**^{1,2} have similar spectral features, with three strong bands at 290, 300, and 311 nm (ε ~ 42–49 × 10^3 M^{-1} cm^{-1}), and an intense shoulder at 335 nm (ε ~ 22 × 10^3 M^{-1} cm^{-1}) assigned by the calculations to intraligand $\pi \rightarrow \pi^*$ transitions in the helicene-NHC-pyridyl ligand. The two weak bands at 376 and 395 nm (ε ~ 6–7×10^3 M^{-1} cm^{-1}) involve transitions from metal and π-helical core to the π-electron system of the helicene-NHC (MLCT and ILCT character respectively). The weaker band at 420 nm (ε ~ 2 × 10^3 M^{-1} cm^{-1}) corresponds to the lowest-energy excitation, and involves the two highest occupied (HO) molecular orbitals (MOs) and the lowest unoccupied (LU) MO, where the HOMO and HOMO-1 are localized on the metal (with visible contributions from the halogen X orbitals) and π-helical moiety, and the LUMO is extended over the π-system of NHC-pyridyl, constituting MLCT, XLCT and ILCT; for relevant MOs, see Figure 3 and Figures S2.9 (**A**^{1}) and S2.10 (**A**^{2}). Re-Cl complexes **B**^{1,2} display similar spectral features to those of **A**^{1,2} but with lower intensities.

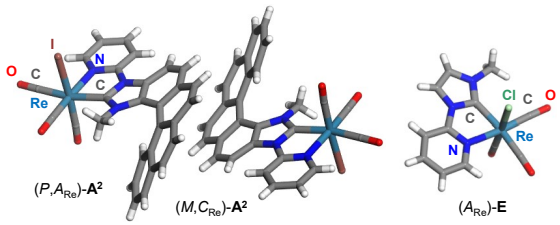

Figure 2. X-ray structures of diastereomerically pure complex **A²** (two enantiomers) and of the enantiopure model system A_{Re}-**E**.

Both pairs of chloro helicene-NHC-Re diastereoisomers **B¹** and **B²** display moderately intense green phosphorescence in deoxygenated solution at ambient temperature, with a well-defined 0,0 vibrational component at 520 nm and a vibronic progression of 1270 cm^{-1} related to helicene C=C stretching. For a summary of photophysical data, see Table 1, and for the corresponding spectra, see SI. The emission is red-shifted compared to that of the model NHC chloro complex **D** (and **E**)[5c] for which λ_{max} = 511 nm (vibrational components are not resolved in those cases), as might be anticipated given the presence of the extended conjugation within the helicene π- system (*vide infra*). Most strikingly, the phosphorescence lifetimes τ_{phos} are vastly increased in the helicene complexes by 4000-6000 times, from 0.1 μs for **D**/**E** to several hundred μs for **B**[1,2]. Indeed, the lifetimes appear to be the longest ever reported for charge-neutral rhenium complexes,[5,17] with only certain cationic systems with aryl isocyanide ligands having comparable lifetimes.[18] Given these high τ_{phos} values, it is not surprising to find that the emission of **B**[1,2] is very efficiently quenched by dissolved molecular oxygen: in air-equilibrated solution, the emission becomes challenging to detect reliably, with τ_{phos} now only around 1 μs. Interestingly, there are subtle differences in τ_{phos} between the diastereoisomers. The **B¹** enantiomers (*M*,A_{Re}) and (*P*,C_{Re}) have lifetimes around 700 μs, whereas for the **B²** pair, (*M*,C_{Re}) and (*P*,A_{Re}), τ_{phos} is around 450 μs (Table 1; note that the estimated uncertainty on τ_{phos} is around ±10%: the small differences between the two enantiomers of each pair are not significant, whereas the difference between the two pairs is). A similar trend emerges for the quantum yields Φ. For both **B¹** and **B²**, the values are higher than for the model systems **D**/**E** (for which Φ = 2.8-3.4%[5b]), but the **B¹** pair emit somewhat more brightly than the **B²** pair (Φ around 9% and 6%, respectively; Table 1).

Assuming that the emitting state is formed with approximately unit efficiency (a reasonable assumption given the good match of excitation spectra with absorption, see SI), the rate constants of radiative k_r and non-radiative Σk_{nr} decay can be estimated from the quantum yields and lifetimes (Table 1). The data provide some insight into the differences between **B**[1,2] *vs.* model systems described above, and also between the diastereoisomeric pairs, **B¹** *vs.* **B²**. The much longer lifetimes of **B**[1,2] compared to **D** are due to large decreases in the rates of both radiative and non-radiative decay. The reduction in k_r is consistent with an excited state that is more closely associated with the large conjugated system of the helicene, with correspondingly less contribution of the metal to promote the spin forbidden $T_1 \rightarrow S_0$ phosphorescence process through spin-orbit coupling. The fact that the quantum yields are only modestly superior to the model complexes, despite the greatly reduced Σk_{nr}, reflects this reduction in k_r. Meanwhile, the rate constant data reveal that the superior quantum yields and longer lifetimes of the **B¹** pair compared to **B²** are due to a reduced rate of non-radiative decay in the former. This presumably reflects the different relative orientations of the halogen with respect to the helicene, with perhaps more protection from the solvent in the **B¹** case, where the halogen is oriented towards the helicene. The degree of protection from the solvent has previously been shown to be important in influencing non-radiative decay in other luminescent Re(I) systems.[17,19] At low temperature (in a frozen glass at 77 K), the emission spectra of **B**[1,2] display more defined vibrational structure, though with only a small blue shift of a few nm, and lifetimes are increased to around 6 ms, consistent with the excited-state being primarily localized on the rigid, helicene ligand. Under these low temperature conditions where solvent interactions are minimal, no significant differences between the two diasteoromeric pairs are observed.

Similar features are seen for the iodo complexes **A¹** and **A²** (when comparing **A**[1,2] to the model complex **C** and comparing **A¹** with **A²**) but their quantum yields are an order of magnitude lower than for their chloro counterparts, and the lifetimes are an order of magnitude smaller (Table 1, SI). These differences stem from a roughly ten-fold increase in the non-radiative decay rate constant, with k_r essentially unchanged. It again appears that the **A¹** enantiomers (*M*,A_{Re}) / (*P*,C_{Re}) have subtly longer lifetimes than the **A²** pair (*M*,C_{Re}) / (*P*,A_{Re}), though the difference is small. The difference between the chloro and iodo compounds contrasts with that observed in more commonly encountered diimine-based complexes of the type *fac*-Re$X(CO)_3$(N^N). With N^N-coordinating diimines such as bipyridine or 1,4-diazabutadienes, a *decrease* in the rates of radiative and non-radiative decay is observed on going from X = Cl to X = I, as the degree of XLCT character of the emitting T_1 state increases.[20] In the present helicene complexes, the more extended conjugation in the :C^N ligand ensures that it, rather than the halide, continues to play the dominant role in the excited state. Here, the poorer performance of the iodo derivatives is probably related to the stronger propensity of iodide to interact with the solvent environment more efficiently than chloride, perhaps due to its larger size and weaker Re–X bond, facilitating deactivation processes. Such processes will be most efficient when the halide is placed in the opposite direction to the helical NHC ligand, as is the case for the (*M*,C_{Re})/(*P*,A_{Re}) enantiomers.

TD-DFT calculations correctly reproduce changes in the phosphorescence energies for the helicene-based Re-NHC complexes *versus* the models lacking the helicene unit, and the calculations confirm that the effect of the extended π-conjugation in the helical NHC ligand is indeed to induce a change in the character of the T_1 excited state from MLCT in the models to mixed MLCT/XLCT/ILCT in both **A**[1,2] and **B**[1,2], with overall lesser involvement of the metal orbitals (see SI). Therefore, the emission behavior combines features of an organometallic system (room temperature phosphorescence) and a helicene (long lifetime and vibronic structure) with an additional unprecedented chirality influence as shown above. Finally, the results are also interesting to compare with our previously reported helicene-bipyridine-rhenium complexes,[21] which display substantially lower-energy emission in the red region (reflecting the stronger π*-accepting nature of the bipyridine unit), much shorter phosphorescence lifetimes, and generally rather low quantum yields (λ_{em} = 598–680 nm; Φ = 0.13–6%, τ_{phos} = 43-79 μs). These differences emphasize the direct impact of the helicenic NHC ligand and its inherent features on the photophysical properties.[9]

The chiroptical properties (OR, ECD, and CPL) of the Re(I) complexes were also examined. Although **D** and **E** were already characterized in their racemic forms,[5b] neither their pure enantiomers nor their chiroptical activity have been reported so far. The ECD spectra of enantiopure **A**^{1,2} and **B**^{1,2} with *P*-helices in CH_2Cl_2 are depicted in Figure 2, and compared to those for **C**, **D** and **E** in the SI. Each pair of enantiomeric complexes shows mirror-image spectra (see SI). Furthermore, systems with the same stereochemistry [(*P*,C_{Re}) for **A**^{1}/**B**^{1}; (*P*,A_{Re}) for **A**^{2}/**B**^{2}] display very similar fingerprints. (*P*,C_{Re})-**A**^{1} exhibits ECD bands at 246 nm ($\Delta\varepsilon$ = +92 M^{-1} cm^{-1}), 287 (-30), 323 (+35), 338 (+47), and 404 (+3), while (*P*,C_{Re})-**B**^{1} shows an almost identical spectrum, except for the band at 246 nm which appears half as intense (Figure 3). Similarly, (*P*,A_{Re})-**A**^{2} displays ECD bands at 241 nm ($\Delta\varepsilon$ = +38 M^{-1} cm^{-1}), 283 (-47), 314 (+96), 338 (+47), and 375 (+16), while (*P*,A_{Re})-**B**^{2} demonstrates the same signals but of overall significantly lower magnitude, excluding the band at 241 nm. Comparing diastereomeric species (**A**^{1} *vs*. **A**^{2} and **B**^{1} *vs*. **B**^{2}): (*i*) a visible increase / decrease in the ECD intensity can be noticed around 320 and 280 nm / 240 nm when changing the stereochemistry at the metal from that in **A**^{1}/**B**^{1} to that of **A**^{2}/**B**^{2}, being especially pronounced for **A**^{1,2} pair, and (*ii*) a significant difference in the spectral envelopes appears above 360 nm, *i.e.* in the region where the Re stereogenic center is mostly involved in the electronic transitions. All this reflects the impact of the distorted-octahedral rhenium chirality and 'match / mismatch' effect on the overall chiroptical activity of **A**^{1,2}/**B**^{1,2}. In comparison, models **C**, **D** and **E** display much weaker ECD spectra. For instance, (C_{Re})-**D** exhibits active bands at 265 nm ($\Delta\varepsilon$ = +13 M^{-1} cm^{-1}), 288 (-28), 313 (+11), and 375 (+5), which are very similar to those of (C_{Re})-**C** and (C_{Re})-**E**. The experimental specific rotations also reflect clear differences between the **A**^{1} *vs*. **A**^{2} and **B**^{1} *vs*. **B**^{2} epimers (see SI). In particular, (*P*,C_{Re})-**A**^{1} displays a specific rotation of +475° cm^2 g^{-1} at 589 nm, while (*P*,A_{Re})-**A**^{2} exhibits a much higher value (+1100), highlighting again the role of the stereogenic rhenium center in tuning the optical activity. Note that the (A_{Re})-(-)/(C_{Re})-(+) absolute configurations for **C**, **D** and **E** were deduced from the X-ray structure of enantiopure **E**, and used to establish those of **A**^{1,2} and **B**^{1,2}. These findings were then confirmed by TD-DFT ECD calculations. The computed ECD spectra agree very well with the experiments, reproducing the relative and absolute band intensities and the signs. The assignments of the ECD bands according to the most intense calculated excitations (see Figure 3 and SI) are qualitatively the same in each case, namely two MLCT bands, and a combination of $\pi \rightarrow \pi^*$ and ILCT, when going from lowest to highest energy

Table 1. UV-visible and emission data for the helicene-NHC-rhenium complexes **A**^{1,2} and **B**^{1,2} and for the model complexes **C** and **D** (in CH_2Cl_2 at 295 K or in EPA at 77 K).

Complex	Absorption [a] λ_{max} / nm (ε / $M^{-1}cm^{-1}$)	Emission λ_{max} / nm [b]	$\Phi \times 10^2$ [c]	τ_{phos} / µs [d]	k_r / s^{-1} [e]	Σk_{nr} / s^{-1} [e]	Emission at 77 K [f]	
							λ_{max} / nm	τ_{phos} / µs
A^1 (*M*,A_{Re})	291 (48667), 310sh (42561), 380 (6783), 397 (6093), 426sh (1783)	520, 556	0.81	50	160	200000	510, 551, 595, 654sh	7700
A^1 (*P*,C_{Re})	290 (49083), 313sh (42331), 378 (7327), 397 (6339), 425sh (2050)	520, 557	0.78	60	130	170000	510, 551, 595, 653sh	7600
A^2 (*P*,A_{Re})	290 (48224), 310sh (42496), 379 (7156), 397 (6000), 428sh (1811)	520, 555	0.77	43	180	230000	508, 548, 591, 646sh	6500
A^2 (*M*,C_{Re})	290 (50577), 308sh (44607), 378 (7555), 396 (6453), 425sh (2097)	520, 555	0.80	44	180	230000	508, 548, 592, 646sh	6600
B^1 (*M*,A_{Re})	290 (23673), 308 (23644), 377 (4298), 398 (3436)	520, 556	9.1	710	130	13000	507, 547, 591, 645sh	6200
B^1 (*P*,C_{Re})	290 (23072), 308 (22800), 378 (4067), 398 (3310)	520, 556	8.9	680	130	14000	508, 547, 590, 645sh	5900
B^2 (*P*,A_{Re})	291 (22537), 308 (22740), 377 (4266), 396 (3327)	519, 555	7.2	480	150	19000	512, 552, 594	6100
B^2 (*M*,C_{Re})	290 (23978), 307 (24202), 378 (4369), 397 (3451)	520, 555	5.4	410	130	23000	512, 551, 594, 651sh	5400
C	285 (17406), 370 (4067), 415 (1268)	511	0.13	0.11	1.2×	9.0×	458	5.2

						10^4	10^6		
D	***rac***	267 (14940), 284 (15493), 360 (6531)	511	1.5	0.11	1.4×10^5	9.0×10^6	458	4.7

[a] In CH_2Cl_2 at 295 ± 1 K. [b] In deoxygenated CH_2Cl_2 at 295 ± 1 K. For the helicene complexes, $\lambda_{max} = \lambda_{(0,0)}$ in each case, whereas there is no vibrational resolution for **C** and **D** so $\lambda_{(0,0)}$ will be somewhat shorter than λ_{max}. [c] Quantum yields in deoxygenated CH_2Cl_2 at 295 ± 1 K were measured using $[Ru(bpy)_3]Cl_{2(aq)}$ as the standard, for which $\Phi = 0.028$.[22] [d] Phosphorescence lifetime in deoxygenated CH_2Cl_2 at 295 ± 1 K, estimated uncertainty in the values is around ±10%; values for the helicene complexes in air-equilibrated complexes are around 1 μs. [e] Radiative k_r and non-radiative Σk_{nr} decay constants estimated assuming that the emissive triplet state is formed with unitary efficiency such that $k_r = \Phi / \tau$ and $\Sigma k_{nr} = (1-\Phi) / \tau$. [f] In diethyl ether / isopentane / ethanol, 2:2:1, v/v.

(longest to shortest wavelength). For **A²** the second band has mixed MLCT/ILCT character. The more intense ECD for **A²** above ca. 260 nm is due to more pronounced charge transfer from the metal to the helicenic NHC, mainly in excitations #2, and #8 to #14. Furthermore, an additional excitation of **A²**, #22 at 278 nm, involving metal → helicene and metal → NHC transitions, contributes to the ECD band around 280 nm. A complete set of calculated data underlying these assignments, and isosurface plots of the relevant MOs, are provided in the SI.

Finally, the CPL (phosphorescence) spectra of each enantiomeric pair of complexes were recorded in CH_2Cl_2 (see Figures 3f and S1.37 for **A¹,²** and **B¹,²** and Figure S1.38 for **D** and **E**). As can be seen, complexes (P,A_{Re})-**A²**/**B²** display very similar CPL spectra, with g_{lum} values of $+5.3\times10^{-3}$ and $+5.6\times10^{-3}$ at 525 nm, respectively. In contrast, (P,C_{Re})-**A¹**/**B¹** systems exhibit much smaller and negative g_{lum} values at this wavelength (-4.4×10^{-4} and -1.4×10^{-3}). Interestingly, the g_{lum} of epimer **A²** is 12 times larger than that of **A¹**, revealing a strong 'match / mismatch' effect imposed by the helix and metal stereochemistries. It is evident that the manipulation of the Re(I) stereochemistry enables the CPL response to be optimized. For comparison, g_{lum} values of $+2.1\times10^{-3}$ and $+1.4\times10^{-3}$ at 523 nm were measured for (C_{Re})-(+)-**D** and (C_{Re})-(+)-**E**, respectively, while no CPL activity could be measured for complex **C**, probably due to its emission being very weak.

In summary, we reported the first enantiopure helicene-NHC-based Re(I) complexes. They exhibit strong chiroptical activity, especially intense circularly polarized phosphorescence, with a 'match / mismatch' effect depending on the stereochemistry of the helicene and of the chiral metal center. Intriguingly, phosphorescence lifetimes >4000 times longer than other NHC and helicene-based Re complexes are observed, reaching values up to 0.7 ms, close to those of lanthanide complexes.[23] Furthermore, we have shown that the identity of the halogen and its stereochemical environment greatly influence the quantum yields and phosphorescence lifetimes. The stereochemistry of transition metal complexes is indeed essential to control the underlying photophysical properties they display. Finally, considering the attraction of Re(I) complexes in electroredox and photoredox activity, appealing applications of such systems as chiral catalysts may be targeted in the future.[5d,e]

Acknowledgements

We thank the Centre National de la Recherche Scientifique (CNRS) and the University of Rennes. This work was supported by the Agence Nationale de la Recherche (ANR-16-CE07-0019 “Hel-NHC” grant, ANR-15-CE30-0005-01 “PVCM” grant). J.A. acknowledges the Center for Computational Research (CCR)[24] for computational resources, and grant CHE-1855470 from the National Science Foundation for financial support. M.S.H. thanks the PL-Grid Infrastructure and the ACC Cyfronet AGH in Krakow, Poland for providing computational resources.

Keywords: helicene, N-heterocyclic carbene, rhenium(I), long-lived phosphorescence, circularly polarized emission

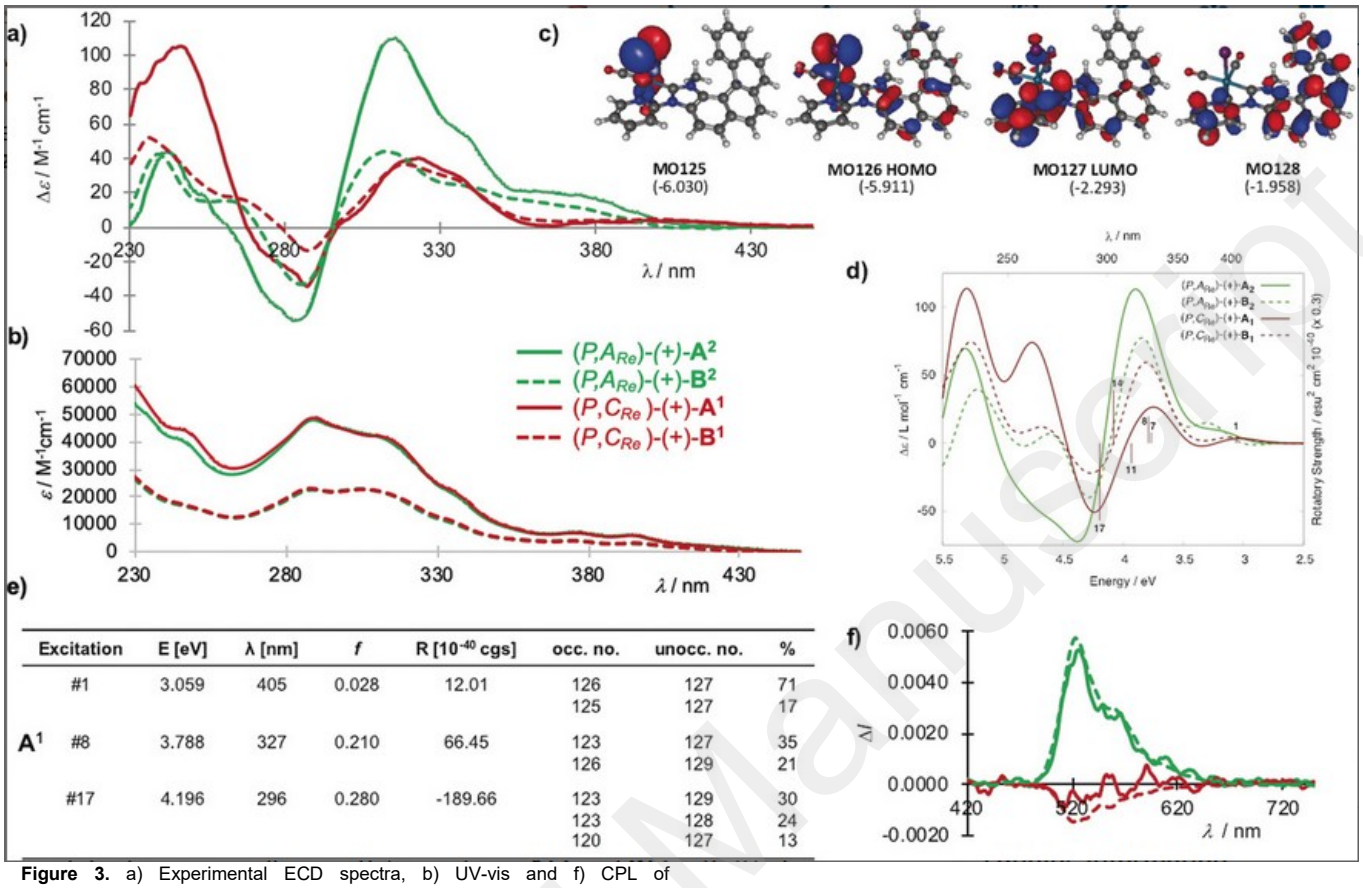

	Excitation	E [eV]	λ [nm]	*f*	R [10^{-40} cgs]	occ. no.	unocc. no.	%
	#1	3.059	405	0.028	12.01	126	127	71
						125	127	17
A¹	#8	3.788	327	0.210	66.45	123	127	35
						126	129	21
	#17	4.196	296	0.280	-189.66	123	129	30
						123	128	24
						120	127	13

Figure 3. a) Experimental ECD spectra, b) UV-vis and f) CPL of enantiomerically and diastereomerically pure Re(I) complexes **A**[1,2] and **B**[1,2] with *P* helices (in CH_2Cl_2 at a concentration of c.a. 10^{-4} M, λ_{ex} = 400 nm). c) Selected MOs involved in the electronic transition of complex **A**[1]. d) Calculated ECD spectra of **A**[1,2] and **B**[1,2] with selected transitions for **A**[1] indicated as 'stick spectra'. e) Selected electronic transitions exhibiting strong rotational strengths.

[1] a) D. Bourissou, O. Guerret, F. P. Gabbai, G. Bertrand, G. *Chem. Rev*. **2000**, *100*, 39-91; b) S. Díez-González (Ed.), *N-Heterocyclic Carbenes: From Laboratory Curiosities to Efficient Synthetic Tools*; RSC: Cambridge, UK; **2011**; c) M. N. Hopkinson, C. Richter, M. Schedler, F. Glorius, *Nature* **2014**, *510*, 485-496.

[2] a) S. Dıez-Gonzalez, N. Marion, S. P. Nolan, *Chem. Rev*. **2009**, *109*, 3612-3676; b) V. César, S. Bellemin-Laponnaz, L. H. Gade, *Chem. Soc. Rev.* **2004**, *33*, 619-636; c) F. Wang, L.-J. Liu, W. Wang, S. Li, M. Shi, *Coord. Chem. Rev.* **2012**, *256*, 804-853; d) D. Zhao, L. Candish, D. Paul, F. Glorius, *ACS Catal.* **2016**, *6*, 5978-5988.

[3] a) M. Mercs, M. Albrecht, *Chem. Soc. Rev.* **2010**, *39*, 1903-1912; b) R. Visbal, M.C. Gimeno, *Chem. Soc. Rev.* **2014**, *43*, 3551-3574; c) C. A. Smith, M. R. Narouz, P. A. Lummis, I. Singh, A. Nazemi, C. -H. Li, C. M. Crudden, *Chem. Rev.* **2019**, *119*, 4986-5056.

[4] a) Y. Unger, D. Meyer, T. Strassner, *Dalton Trans*. **2010**, *39*, 4295-4301; b) T. Sajoto, P. I. Djurovich, A. Tamayo, M. Yousufuddin, R. Bau, M. E. Thompson, R. J. Holmes, R. S. Forrest, *Inorg*. *Chem*. **2005**, *44*, 7992-8003; c) S. U. Son, K. H. Park, Y.-S. Lee, B. Y. Kim, C. H. Choi, M. S. Lah, Y. H. Jang, D.-J. Jang, Y. K. Chung, *Inorg*. *Chem*. **2004**, *43*, 6896-6898; d) D. Di, A. S. Romanov, L .Yang, J. M. Richter, J. P. H. Rivett, S. Jones, T. H. Thomas, M. A. Jalebi, R. H. Friend, M. Linnolahti, M. Bochmann, D. Credgington, *Science* **2017**, *356*, 159-163; e) R. Hamze, S. Shi, S. C. Kapper, D. S. M. Ravinson, L. Estergreen, M. -C. Jung, A. C. Tadle, R. Haiges, P. I. Djurovich, J. L. Peltier, R. Jazzar, G. Bertrand, S. E. Bradforth, M. E. Thompson, *J. Am. Chem. Soc.* **2019**, *141*, 21, 8616-8626; f) R. Hamze, J. L. Peltier, D. Sylvinson, M. Jung, J. Cardenas, R. Haiges, M. Soleilhavoup, R. Jazzar, P. I. Djurovich, G. Bertrand, M. E. Thompson, *Science* **2019**, *363*, 601-606; g) M. Deng, N. F. M. Mukthar, N. D. Schley, G. Ung. *Angew. Chem. Int. Ed.* **2019,** DOI: 10.1002/anie.201913672; h) H. Tatsuno, *et al. Angew. Chem. Int. Ed.* **2020**, *59*, 364-372.

[5] a) L. A. Casson, S. Muzzioli, P. Raiteri, B. W. Skelton, S. Stagni, M. Massi, D. H. Brown, *Dalton Trans*. **2011**, *40*, 11960-11967; b) X.-W. Li, H.-Y. Li, G.-F. Wang, F. Chen, Y.-Z. Li, X.-T. Chen, Y.-X. Zheng, Z.-L. Xue, *Organometallics* **2012**, *31*, 3829-3835; c) J. G. Vaughan, B. L. Reid, S. Ramchandani, P. J. Wright, S. Muzzioli, B. W. Skelton, P. Raiteri, D. Brown, S. Stagni, M. Massi, *Dalton Trans.* **2013**, *42*, 14100-14114; d) C. J. Stanton, III, C. W. Machan, J. E. Vandezande, T. Jin, G. F. Majetich, H. F. Schaefer, III, C. P. Kubiak, G. Li, J. Agarwal, *Inorg. Chem.* **2016**, *55*, 3136-3144; e) A. J. Huckaba, E. A. Sharpe, J. H. Delcamp, *Inorg. Chem.* **2016**, *55*, 682-690.

[6] P. V. Simpson, M. Falasca, M. Massi, *Chem. Commun.* **2018**, *54*, 12429-12438.

[7] a) H. Isla, J. Crassous, *C. R. Chimie* **2016**, *19*, 39-49; b) J.-K. Ou-Yang, J. Crassous*, Coord. Chem. Rev*. **2018**, *376*, 533-547; c) K. Dhbaibi, L. Favereau, J. Crassous, *Chem. Rev.* **2019**, ***119***, 8846-8953.

[8] C.-F. Chen, Y. Shen, 'Helicene Chemistry: From Synthesis to Applications'; Springer Berlin Heidelberg: Berlin, Heidelberg, **2017**.

[9] a) N. Hellou, M. Srebro-Hooper, L. Favereau, F. Zinna, E. Caytan, L. Toupet, V. Dorcet, M. Jean, N. Vanthuyne, J. A. G. Williams, L. Di Bari, J. Autschbach, J. Crassous, *Angew. Chem. Int. Ed.* **2017**, *56*, 8236-8239; b) A. Macé, N. Hellou, J. Hammoud, C. Martin, E. S. Gauthier, L. Favereau, T. Roisnel, E. Caytan, G. Nasser, N. Vanthuyne, J. A. G. Williams, F. Berrée, B. Carboni, J. Crassous, *Helv. Chim. Acta* **2019**, *102*, e1900044.

[10] H. Zhang, Q. Cai,D. Ma, *J. Org. Chem*. **2005**, *70*, 5164-5173.

[11] a) A. von Zelewsky, *Stereochemistry of Coordination Compounds*, J. Wiley & Sons, Chichester, **1996**; b) V. I. Sokolov, *Chirality and Optical Activity in Organometallic Compounds*, Gordon & Breach Science Publishers, New York, **1990**; c) A. Amouri, M. Gruselle, *Chirality in Transition Metal Chemistry: Molecules, Supramolecular Assemblies and Materials*, Wiley-VCH, **2009**

[12] a) M. P. Mitoraj, A. Michalak, T. Ziegler, *J. Chem. Theory Comput.* **2009**, *5*, 962-975; b) M. Srebro, A. Michalak, *Inorg. Chem*. **2009**, *48*, 5361-5369.

[13] M. J. Frisch, G. W. Trucks, H. B. Schlegel *et al*. "Gaussian 16, Revision B.01", Gaussian, Inc., Wallingford CT, 2016. URL: www.gaussian.com.

[14] A. D. Becke, *J. Chem. Phys.* **1993**, *98*, 5648-5652.

[15] a) F. Weigend, R. Ahlrichs, *Phys. Chem. Chem. Phys.* **2005**, *7*, 3297-3305; b) F. Weigend, *Phys. Chem. Chem. Phys.* **2006**, *8*, 1057-1065.

[16] G. Scalmani, M. J. Frisch, *J. Chem. Phys.* **2010**, *132*, 114110.

[17] L. A. Sacksteder, M. Lee, J. N. Demas, B. A. De Graff, *J. Am. Chem. Soc.* **1993**, *115*, 8230-8238.

[18] J. M. Favale, Jr., E. O. Danilov, J. E. Yarnell, F. N. Castellano, *Inorg. Chem.* **2019**, *58*, 8750-8762.

[19] M. P. Coogan, V. Fernández-Moreira, J. B. Hess, S. J. A. Pope and C. Williams, *New J. Chem.* **2009**, *33*, 1094-1099.

[20] B. D. Rossenaar, D. J. Stufkens and A. Vlcek, *Inorg. Chem.* **1996**, *35*, 2902-2909.

[21] N. Saleh, M. Srebro, T. Reynaldo, N. Vanthuyne, L. Toupet, V. Y. Chang, G. Muller, J. A. G. Williams, C. Roussel, J. Autschbach, J. Crassous, *Chem. Comm.* **2015**, ***51***, 3754-3757.

[22] K. Nakamaru, *Bull. Chem. Soc. Jpn*. **1982**, *55*, 2697.

[23] P. Hänninen, H. Härmä, (Eds.) Lanthanide Luminescence: Photophysical, Analytical and Biological Aspects, Springer Series on Fluorescence, **2011**.

[24] Center for Computational Research, University at Buffalo, http://hdl.handle.net/10477/79221